Applied Physics B (2018) 124:4
https://doi.org/10.1007/s00340-017-6874-9

Applied Physics B
Lasers and Optics

RAPID COMMUNICATION

All-fiber high-power monolithic femtosecond laser at 1.59 µm with 63-fs pulse width

M. J. Hekmat[1] · M. Omoomi[1] · A. Gholami[1] · A. Bagheri Yazdabadi[1] · M. Abdollahi[1] · E. Hamidnejad[1] · A. Ebrahimi[1] · H. Normohamadi[1]

Received: 24 October 2017 / Accepted: 5 December 2017 / Published online: 11 December 2017

Abstract
In this research, by adopting an alternative novel approach to ultra-short giant pulse generation which basically originated from difficulties with traditional employed methods, an optimized Er/Yb co-doped double-clad fiber amplifier is applied to boost output average power of single-mode output pulses to a high level of 2-W at 1.59-µm central wavelength. Output pulses of approximately 63-fs pulse width at 52-MHz repetition rate are obtained in an all-fiber monolithic laser configuration. The idea of employing parabolic pulse amplification for stretching output pulses together with high-power pulse amplification using Er/Yb co-doped active fibers for compressing and boosting output average power plays crucial role in obtaining desired results. The proposed configuration enjoys massive advantages over previously reported literature which make it well-suited for high-power precision applications such as medical surgery. Detailed dynamics of pulse stretching and compressing in active fibers with different GVD parameters are numerically and experimentally investigated.

1 Introduction

Recently, all-fiber femtosecond lasers have been attracting considerable attention. For several applications such as THz generation [1], direct writing [2], bio-photonics [3, 4], spectroscopy [5] and micromachining [6], FBG fabrication [7], and medicine [8], robust femtosecond fiber lasers enjoy definite advantages over their solid-state peer, Ti:Sa ultra-short pulsed lasers. Chirped pulse amplification (CPA) using erbium (Er)- or ytterbium (Yb)-doped active fibers has made substantial progress in recent years, despite the fact that the obtainable output power is highly restricted by the maximum pump power that can be coupled into the gain fiber without causing optical damage or nonlinear pulse distortion [9–14]. In CPA approach by means of all-fiber stretchers or solid-state prism/gratings, optical pulses are stretched to picosecond regimes before amplification and after that amplified, output pulses are compressed. GVD and other nonlinear effects do not play central roles in this method. Due to the high conversion efficiency, CPA methods are typically implemented in Yb-doped fiber amplifiers [9, 15], but a few reports are available with special Er-doped fiber amplifiers [16, 17]. Er-doped fiber amplifiers operating at 1.5-µm central wavelength are not highly efficient in producing high-power output pulses inasmuch as they suffer from clustering effects in Erbium ions [18]. Moreover, several other reports are available in the literature in which Er/Yb co-doped fiber amplifiers have been employed [19, 20]. In these reports, CPA methods have not been adopted in all-fiber monolithic configurations and as a result the stability of operation is highly dependent on environmental variations making them inappropriate for practical applications. Another approach commonly employed to ultra-short giant

✉ M. J. Hekmat
m.hekmat@ec.iut.ac.ir

M. Omoomi
omoomi@cc.iut.ac.ir

A. Gholami
gholami@cc.iut.ac.ir

A. Bagheri Yazdabadi
a.bagheri@grad.kashanu.ac.ir

M. Abdollahi
mo.abdollahi@sci.ui.ac.ir

E. Hamidnejad
ehsan.hamidnejad@ec.iut.ac.ir

A. Ebrahimi
ali.ebrahimi67@payammail.ir

H. Normohamadi
hosein.normohamadi@gmail.com

[1] Department of Electrical and Computer Engineering, Isfahan University of Technology, Isfahan 8415683111, Iran

pulse generation is parabolic pulse amplification [21–24]. Optical pulses propagating through normal dispersion fiber amplifiers will turn into linearly chirped parabolic pulses at the same time when they are amplified [25]. These pulses afterwards can be effectively compressed by propagating through optical fibers in anomalous dispersion regime. Two important advantages are worth mentioning regarding this approach. First, it has been shown that parabolic optical pulses are approximately wave-breaking-free solutions of the nonlinear Schrodinger equation in the high-intensity regimes [26–29]. Second, the output pulse shape of amplified pulses in the normal GVD regime is almost independent of the input pulse shape.

In the present study by considering the aforementioned points, an innovative novel approach is adopted to high-power ultra-short pulse generation by making use of parabolic pulse amplification and high-power pulse amplification in Er/Yb co-doped fiber amplifiers. In the proposed configuration, fiber amplifiers are employed as pulse stretcher/compressor components while at the same time boost the output average power of optical pulses, resulting in a truly monolithic and compact all-fiber configuration generating shorter high-power ultra-short optical pulses when compared to the previously reported literature. Since Er/Yb co-doped fiber amplifiers offer distinguishing features of wide gain bandwidth and high-power output average powers [27], appropriately designed fiber amplifiers can at the same time act as stretcher/compressor components while boosting the output average power of optical pulses. A negative dispersion Er/Yb co-doped fiber amplifier is applied for pulse compressing and de-chirping of amplified pulses which were amplified in the normal GVD regime of the pre-amplifier stage. Output pulses of approximately 63-fs pulse width at 52.27-MHz repetition rate are obtained in this approach which is pulse-breaking-free with 34-nj pulse energy and 2-W average power at 1.59-μm central wavelength. This new configuration is theoretically and experimentally investigated for different amount of input pump power in the Er/Yb co-doped fiber amplifier and obtained experimental results show good consistency with predicted theoretical ones.

2 Theoretical model

A schematic configuration of the proposed ultra-short high-power fiber laser is shown in Fig. 1. This Master Oscillator Power Amplifier (MOPA) configuration consists of an Er-doped fiber amplifier in the pre-amplification stage which is seeded by an Er-doped fiber laser oscillator and acts as a pulse stretcher in the normal GVD regime, and an Er/Yb co-doped fiber amplifier in the high-power amplification stage acting as a pulse compressor, while at the same time fiber amplifiers are employed to boost

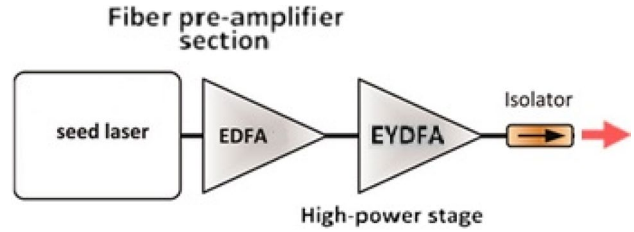

Fig. 1 Schematic configuration of ultra-short high-power fiber laser

output average powers. At the end of boost fiber amplifier, an optical fiber isolator is applied to suppression of any ASE back reflection from the end face of output boost amplifier.

To simulate ultra-short pulse width propagation in fiber amplifiers, input pulse characteristics are used as starting points and after propagation through the amplifier, output pulse characteristics such as pulse width and pulse spectrum are obtained. Ultra-short pulse propagation in optical fibers by considering different effects of gain, loss, dispersion and fiber nonlinearity is given by the nonlinear schrodinger equation (NLSE) [30]:

$$i\frac{\partial U}{\partial z} - \frac{1}{2}\beta_2\frac{\partial^2 U}{\partial t^2} + \gamma|U|^2U = i(g - \Gamma)U \tag{1}$$

where $U = U(z, t)$ is the electromagnetic field envelope, z is the propagation direction along the fiber, t is the time frame, β_2 ($ps^2\ m^{-1}$) is the group velocity dispersion coefficient, γ ($W^{-1}\ m^{-1}$) is the nonlinear coefficient and Γ (dB/m) is the linear loss coefficient. By considering gain non uniformity along the entire fiber length, one can see that gain dynamics inside an Er-doped fiber amplifier is given by [31]:

$$\frac{\partial g(z,\ t)}{\partial t} = \frac{g_0 - g(z,\ t)}{\tau_g} - \frac{g(z,\ t)|U\ (z,\ t)|^2}{P_{s,g}\tau_g} \tag{2}$$

where g_0 (dB m^{-1}) is the small signal gain, τ_g (μs) is the inversion relaxation time and $P_{s,g}$ (mW) is the saturation power of the gain medium. Some of these key parameters required for simulation, have been measured for commonly used rare-earth-doped optical fibers and are available in Ref [31]. These parameters are heavily dependent on the fabrication process and may differ from one to the other. In an ultra-short fiber amplifier, the gain relaxation time is much longer than the pulse width T_0 ($T_0 \ll \tau_g$) and, therefore, it does not change significantly over a single pulse propagation. Thus, we can assume $\frac{\partial g(z,\ t)}{\partial t} = 0$ and it will be saturated for high-intensity input pulses. These two coupled equations are integrated by the Split Step method to simulate ultra-short pulse propagation through passive and active optical components [30]. Our simulations are divided into two stages, pulse stretching in normal GVD regime by propagating through the Er-doped fiber amplifier and pulse compressing in anomalous dispersion regime by propagating through the Er/Yb co-doped fiber amplifier. Some of the important parameters used in simulations are given in Table 1. Ultra-short pulse propagation through normal GVD fiber amplifiers was thoroughly discussed in [25]. Suitable input pulse width, pulse energy and active fiber length are needed for parabolic pulse amplification. Output pulse shapes of parabolic fiber amplifiers are independent of input pulses and as a result, femtosecond fiber lasers based on MOPA configurations enjoy great advantages over commonly used CPA methods. Based on our simulations, it is seen that an approximately 6-m long Er-doped fiber amplifier would be suitable for achieving parabolic pulse amplification in the pre-amplification stage. Temporal profiles of input and output-amplified pulses in the pre-amplification stage are shown in Fig. 2a.

In a parabolic pulsed fiber amplifier, slightly positive-chirped input pulses are much desirable than non-chirped input pulses and even will reduce the optimized fiber length of the parabolic fiber amplifier. Output spectra of the pre-amplification stage in the normal GVD regime for different input chirped pulses are shown in Fig. 2c. As it can be seen in Fig. 2a, when pulse propagates in a normal GVD optical fiber, pulse broadening in both time and frequency domains is observed. After input pulses are amplified and stretched to a few picoseconds. In the pre-amplification stage, output pulse characteristics are used as starting points for power amplifier simulations in the anomalous dispersion regime. Temporal profile of the output pulses after power amplifier stage is shown in Fig. 2b. Compressed pulses can be achieved in this power amplifier.

3 Experimental setup and discussion

A schematic diagram of the applied MOPA configuration is shown in Fig. 3. The Er-doped fiber amplifier in the pre-amplification stage is seeded by a normal dispersion, Er-doped fiber laser mode-locked by a commercial SESAM. The normal dispersion cavity design in the master oscillator has resulted in the broadest output spectrum and slightly positive-chirped output pulses and it is beneficial for achieving parabolic pulse amplification in the pre-amplification stage. This master oscillator is designed for generating output pulses with desired characteristics regarding the pre-amplification stage.It consists of a 98-cm long Er-doped fiber developed by the Liekki, Er80-4/125, with nominal absorption coefficient of 80-dB/m at 1530-nm and normal group velocity dispersion. Other passive components used in the cavity were standard single-mode optical fibers (SMFs) and HI1060 with a GVD value of about 17- and 6-ps/nm/km, respectively, with total passive length of about 30-cm. The laser cavity was pumped by a 400-mW laser diode at the central wavelength of 980-nm. A 20/80 fiber coupler was used to provide the laser output. The applied SESAM (BATOP GmbH) is based on InGaAs quantum wells. It has a saturable absorption modulation depth of about 30%, a saturation fluence of about 70-μJ/cm^2 and a recovery time of about 2-ps. The pre-amplification stage consists of a 5.8-m long normal GVD Er-doped active fiber with $\gamma = 3.6$-W^{-1} km^{-1} and $\beta_2 = 12.5$ ps^2/km bi-directionally pumped through two 976-nm single-mode 500 mW pump laser diodes. Based on our simulations, the optimized length of the active fiber for achieving parabolic pulse amplification is around 5.8-m and it plays a crucial role in the amplification process (see Sect. 2). In the power amplification stage, pulses are boosted to about 2-W average power through a double-clad Er/Yb co-doped active fiber with core/cladding diameters of 12/130-μm. The active fiber is pumped by a 12-W multimode laser diode at 972-nm central wavelength in the forward-pumping configuration through a $(1+1)\times 1$ home-made side-pump fiber combiner. Backward-propagating radiation from the high-power amplification stage is monitored and suppressed by inserting a circulator before this stage. To remove spurious lasing, output facet of the passive fiber at the output of boost amplifier is angle cleaved which leads to higher damage threshold at high-level output average powers. The master oscillator generates output pulses of approximately 360-fs pulse width at the central wavelength of 1560-nm

Table 1 Key parameters used in simulations

Symbols	Quantity	Pulse stretcher stage	Pulse compressor stage
λ_0	Input central wavelength	1560 nm	1560 nm
P_0	Input average power	10 mW	240 mW
T_0	Input pulse width	350 fs	1350 fs
g	Amplifier gain	2/m	2/m
L	Fiber length	2–6 m	3–4 m
γ	Nonlinear coefficient	3.6 W^{-1}km^{-1}	3 W^{-1}km^{-1}
β_2	Group velocity dispersion coefficient	12.5 ps^2/km	20.5 ps^2/km
U_0	Input pulse shape	sech^2	Parabolic
C	Input chirp parameter	2–8	30–50

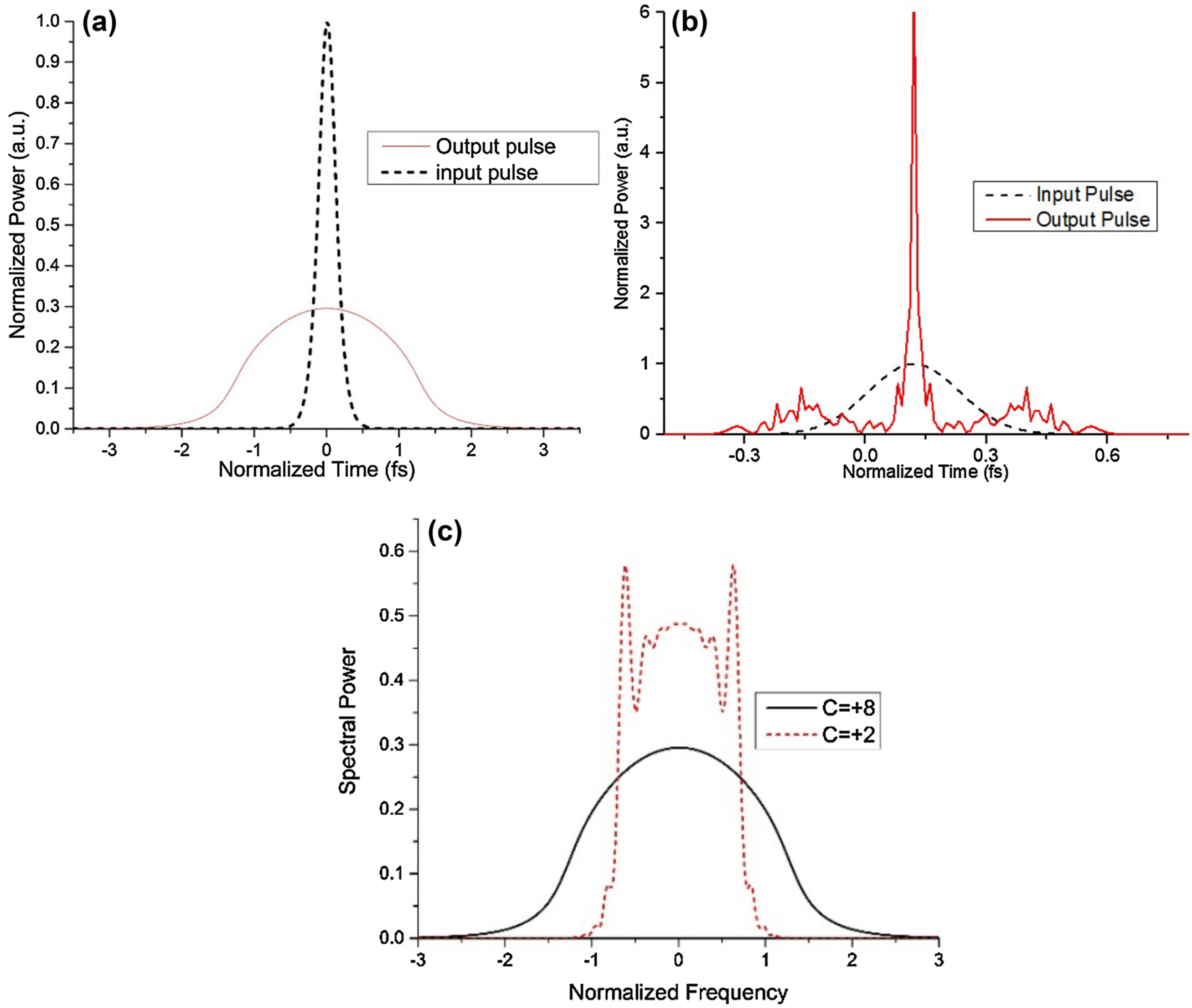

Fig. 2 Simulated temporal profiles of output pulses after, **a** pre-amplifier stage as a pulse stretcher and **b** Er/Yb co-doped power amplifier stage as pulse compressor. **c** Effect of cavity chirp on output spectra of the parabolic fiber amplifier

with a 9-nm bandwidth (FWHM).Its measured optical spectrum has a soliton-like shape with some Kelly sidebands which are not in excess of a few. The autocorrelation profile of output pulses is of a $sech^2$ pulse shape. The output power is ~10-mW for the input pump power of 150-mW which is corresponded to the output pulse energy of 191-pJ. In the pre-amplifier stage, optical pulses are amplified while at the same time an extra frequency chirping is added to them. The overall amplification factor provided by this stage is around 24 which results in output pulses with approximately 1.32-ps pulse width, 26-nm spectral bandwidth and ~240-mW average power. These output pulses are large enough to induce a strong growth of the peak power in the main amplifier stage. In the main amplifier, output pulses of maximum average power of approximately 2-W are generated at ~52-MHz repetition rate. Figure 4 shows output optical spectra and temporal autocorrelation profiles versus different output average powers in the main amplifier stage. By increasing output average power, output pulse width is reduced from 400- to 63-fs. The remaining amount of chirping is completely compressed in an 87-cm long single-mode passive matched fiber. This passive component completely compresses output pulses from the main amplifier stage at the maximum output average power. Above 1.2-W output average power, the temporal pulse width stays constant around 63-fs. By comparing Fig. 4b with Fig. 2b, one can see that experimental results are in good consistency with predicted numerical simulation.

Measured output characteristics including an example pulse train below than 25-ns temporal spacing and the

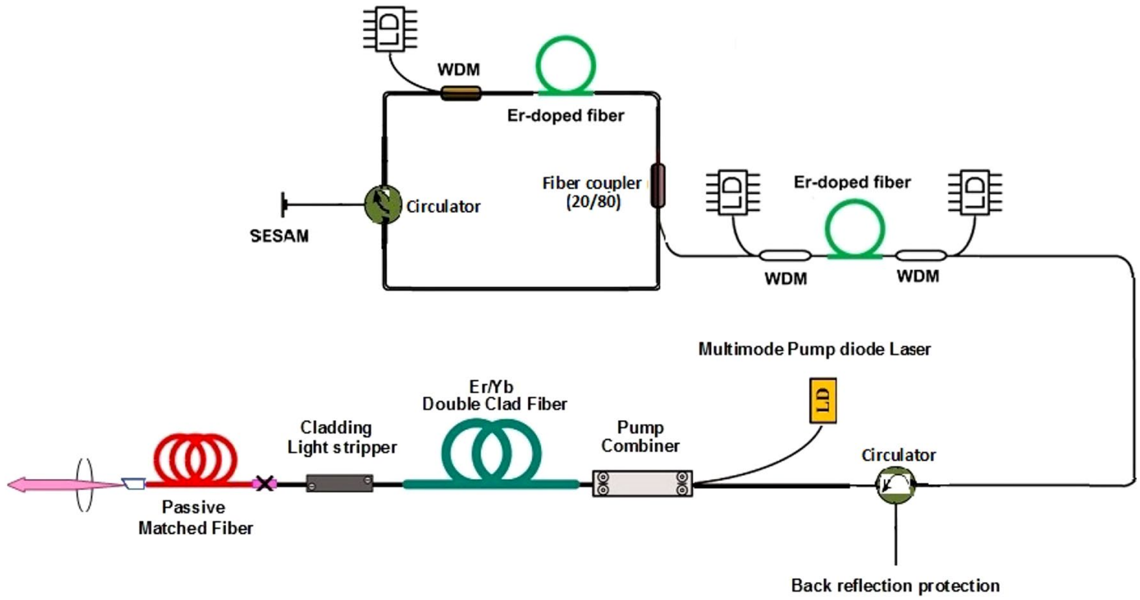

Fig. 3 Schematic configuration of the employed ultra-short high-power MOPA system. *SESAM* semiconductor saturable absorber mirror, *LD* laser diode, *WDM* wavelength division multiplexer

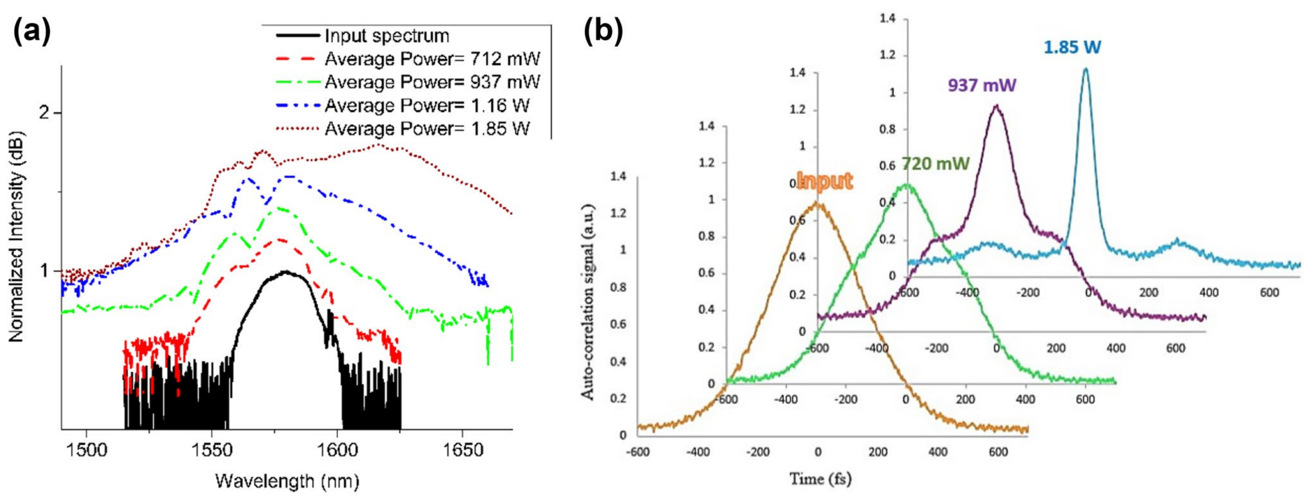

Fig. 4 Output pulse characteristics vs different output average powers at 52.27 MHz: **a** optical spectra and **b** temporal autocorrelation profiles

corresponding RF spectrum are shown in Fig. 5. It can be seen that up to five harmonics orders are observed in the RF spectrum of a 52.27 MHz repetition rate and its signal-to-noise ratio (SNR) at 100 kHz resolution bandwidth (RBW) is approximately around 60-dB. As it can be seen, output of power amplifier was operated in pulse-breaking-free regime and only harmonics of center frequency appeared at the electrical spectrum (ES) The output pulse width in the temporal domain was measured using an autocorrelator (Femtochrome Research FR-103PD) and was estimated to be 63-fs and the corresponding full width at half maximum (FWHM) in the spectral domain was about 63-nm (measured by optical spectrum analyzer ADVANTEST Q8384). Long-term stable operation was tested for a period of 4 h with the best stable results ever seen. The stability of fiber amplifier is observed for both output average power and autocorrelator pulse trace and are shown in Fig. 6.

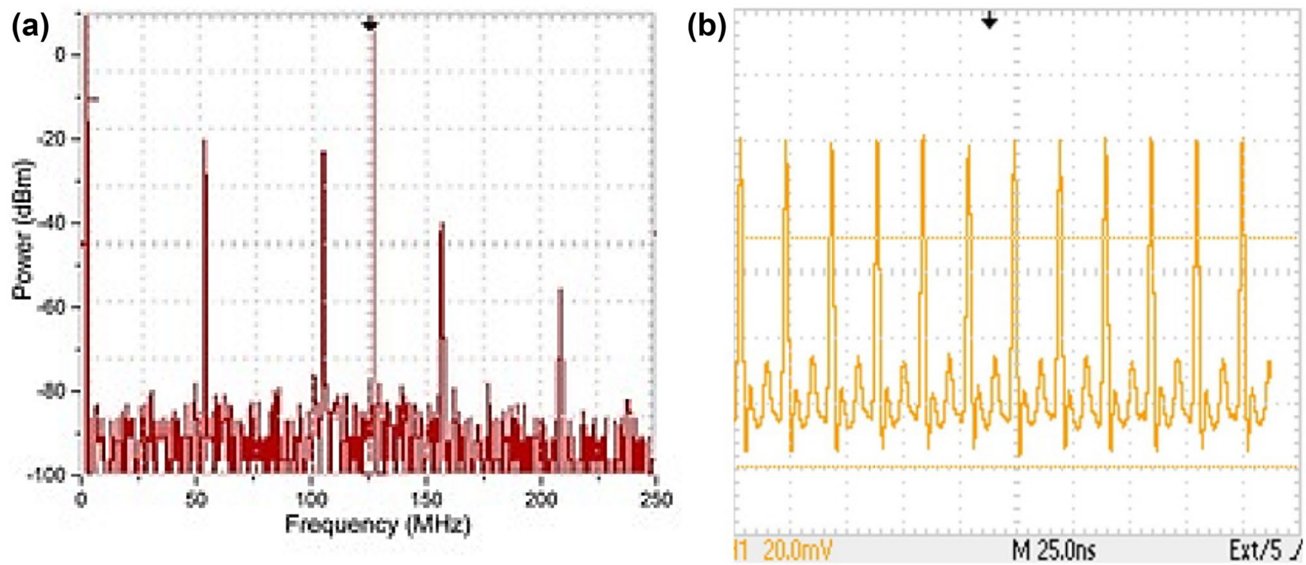

Fig. 5 Temporal characteristics of output pulses. **a** RF spectrum, **b** output pulse train

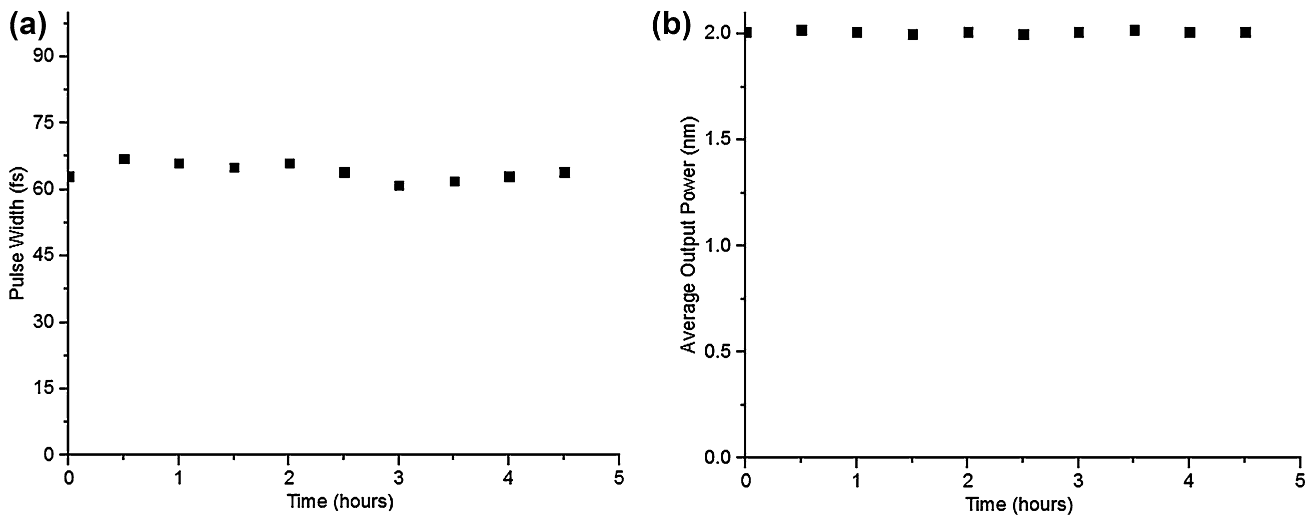

Fig. 6 **a** Pulse width stability and **b** output average power stability in the period of time

4 Conclusion

We have demonstrated a stable mode-locked ultra-short fiber laser in the master oscillator power amplifier configuration. In our study, by making use of nonlinear effects rather than simply throwing them away, highly stable ultra-short giant pulses are generated in an all-fiber monolithic robust configuration. In this approach, different amplification stages act as pulse stretcher/compressor at the same time while they boost output average powers. Our configuration provides stable and cost-effective ultra-short giant pulses which are well-suited for commercial applications. Self-starting and stable mode-locked ultra-short pulses at a repetition rate of 52.23-MHz are generated. Output pulses with 63-fs pulse width at the central wavelength of 1590-nm and approximately 63-nm bandwidth are generated in a monolithic all-fiber configuration. Detailed dynamics of pulse stretching and compressing in active fibers with different GVD parameters are numerically and experimentally investigated. We have shed light on the benefits of employing fiber amplifiers as pulse stretcher/compressor components.

References

1. L. Jiang, et al., Efficient terahertz wave generation from GaP crystals pumped by chirp-controlled pulses from femtosecond photonic crystal fiber amplifier. Appl. Phys. Lett. **104**, 031117 (2014)
2. J.R. Grenier, et al., Femtosecond laser fabrication of phase-shifted Bragg grating waveguides in fused silica. Opt. Lett. **37**(12):2289–2291 (2012)
3. M.S. Bello-Silva, M. Wehner, C. de Paula Eduardo, F. Lampert, R. Poprawe, M. Hermans, M. Esteves-Oliveira, Precise ablation of dental hard tissues with ultra-short pulsed lasers. Preliminary exploratory investigation on adequate laser parameters. Lasers Med Sci. **28**(1), 171–184 (2013)
4. J. Liu, L. Yang, *Femtosecond Fiber Lasers for Biomedical Solutions. Paper 8551–15, SPIE Photonics Asia* (2012)
5. H. Huang, L.-M. Yang, J. Liu, *Femtosecond fiber laser direct writing of optical waveguide in glasses*. SPIE Paper Number: 8358-43 (2012)
6. B.-W. Liu, M.-L. Hu, X.-H. Fang, Y.-Z. Wu, Y.-J. Song, L. Chai, C.-Y. Wang, A.M. Zheltikov, High-power wavelength-tunable photonic-crystal-fiber-based oscillator-amplifier-frequency-shifter femtosecond laser system and its applications for material microprocessing. Laser Phys. Lett. **6**(1), 44–48 (2009)
7. T. Geernaert, K. Kalli, C. Koutsides, M. Komodromos, T. Nasilowski, W. Urbanczyk, J. Wojcik, F. Berghmans, H. Thienpont, Point-by-point fiber Bragg grating inscription in free-standing step-index and photonic crystal fibers using near-IR femtosecond laser. Opt. Lett. **35**(10), 1647 (2010)
8. M. Braun, P.G.W. Zinth, *Ultrashort Laser Pulses in Biology and Medicine* (Springer-Verlag, Berlin Heidelberg, 2008)
9. T. Eidam, S. Hanf, E. Seise, T.V. Andersen, T. Gabler, C. Wirth, T. Schreiber, J. Limpert, A. Tünnermann, Femtosecond fiber CPA system emitting 830 W average output power. Opt. Lett. **35**, 94–96 (2010)
10. J. Limpert, F. Röser, D.N. Schimpf, E. Seise, T. Eidam, S. Hädrich, J. Rothhardt, C.J. Misas, A. Tünnermann, High repetition rate gigawatt peak power fiber laser systems: challenges, design, and experiment. IEEE J. Sel. Top. Quantum Electron. **15**, 159–69 (2009)
11. T. Eidam, J. Rothhardt, F. Stutzki, F. Jansen, S. Hädrich, H. Carstens, C. Jauregui, J. Limpert, A. Tünnermann, Fiber chirped-pulse amplification system emitting 3.8 GW peak power. Opt. Express **19**, 255–260 (2011)
12. S. Hädrich, H. Carstens, J. Rothhardt, J. Limpert, A. Tünnermann, Multi-gigawatt ultrashort pulses at high repetition rate and average power from two-stage nonlinear compression. Opt. Express **19**, 7546–7552 (2011)
13. S.-P. Chen, H.-W. Chen, Z.-J. Liu, 100 W all fiber picosecond MOPA laser. Opt. Express **17**,24008–24012 (2009)
14. R. Song, S. Hou, W. Yang, Q. Lu, 157 W all-fiber high-power picosecond laser. Appl. Opt. **51**,2497–2500 (2012)
15. L. Kuznetsova, F.W. Wise, Scaling of femtosecond Yb-doped fiber amplifiers to tens of microjoule pulse energy via nonlinear chirped pulse amplification. Opt. Lett. **32**(18), 2671 (2007)
16. X. Peng, K. Kim, M. Mielke, S. Jennings, G. Masor, D. Stohl, A. Chavez-Pirson, D.T. Nguyen, D. Rhonehouse, J. Zong, D. Churin, N. Peyghambarian, High efficiency, monolithic fiber chirped pulse amplification system for high energy femtosecond pulse generation. Opt. Express **21**(21), 25440 (2013)
17. X. Peng, K. Kim, M. Mielke, S. Jennings, G. Masor, D. Stohl, A. Chavez-Pirson, D.T. Nguyen, D. Rhonehouse, J. Zong, D. Churin, N. Peyghambarian, Monolithic fiber chirped pulse amplification system for millijoule femtosecond pulse generation at 1.55 µm. Opt. Express **22**(3), 2459, (2014)
18. B. Morasse, S. Agger, C. Hovington, S. Chatigny, É Gagnon, J. Sandro, C. Poulsen, 10W ASE-free single-mode high-power double-cladding Er3+-Yb3 + amplifier. Proc. SPIE **6453**, 645324 (2007)
19. S. Han, H. Jang, S. Kim, Y.-J. Kim, S.-W. Kim, MW peak power Er/Yb-doped fiber femtosecond laser amplifier at 1.5 µm center wavelength. Laser Phys. Lett. **14**, 080002 (2017)
20. G. Sobon, P.R. Kaczmarek, D. Sliwinska, J. Sotor, K.M. Abramski, High-power fiber-based femtosecond CPA system at 1560 nm. IEEE J. Sel. Top. Quantum Electron **20**, 5 (2014)
21. W. Zhao, X. Hu, Y. Wang, Femtosecond-pulse fiber based amplification techniques and their applications. IEEE J. Sel. Top. Quantum Electron., **20**, 5, (2014)
22. M.E. Fermann, Self-similar propagation and amplification of parabolic pulses in optical fibers. Phys. Rev. Lett. **84**, 26 (2000)
23. A. Ruehl, O. Prochnow, D. Wandt, D. Kracht, Dynamics of parabolic pulses in an ultrafast fiber laser. Opt. Lett **31**(18), 15 (2006)
24. B. Kibler, C. Billet, P.-A. Lacourt, R. Ferriere, J. M. Dudley, All-fiber source of 20-fs pulses at 1550 nm using two-stage linear–nonlinear compression of parabolic similaritons. IEEE Photon. Technol. Lett. **18**, 17 (2006)
25. V.I. Kruglov, A.C. Peacock, J.D. Harvey, Self-similar propagation of parabolic pulses in normal-dispersion fiber amplifiers. J. Opt. Soc. Am. B **19**, 3 (2002)
26. D. Anderson, M. Desaix, M. Karlsson, M. Lisak, M.L. Quiroga-Teixeiro, Wave-breaking-free pulses in nonlinear-optical fibers. J. Opt. Soc. Am. B **10**(7), 1185, (1993)
27. R. Ahmad, S. Chatigny, M. Rochette, Broadband amplification of high power 40 Gb/s channels using multimode Er-Yb doped fiber. Opt. Express **18**(19),19983, (2010)
28. G. Sobon, P. Kaczmarek, A. Gluszek, J. Sotor, K.M. Abramski, µJ-level, kHz-repetition rate femtosecondfiber-CPA system at 1555 nm. Opt. Commun. **347**(8), 12 2015
29. V. Roy, L. Desbiens, Y. Taillon, All-fiber, high power, rugged ultrashort-pulse laser source at 1550 nm. Proc. SPIE **7386**, 738633–738631 (2009)
30. G. Agrawal, *Nonlinear Fiber Optics* (Academic press, New York, 2013)
31. O.G. Okhotnikov, *Fiber Lasers* (Wiley-VCH Verlag & Co. KGaA, New York, 2012)